Cao, Yan; Li, Yiqing; Zhang, Geng; Kittisak Jermsittiparsert; Razmjooy, Navid

Article

Experimental modeling of PEM fuel cells using a new improved seagull optimization algorithm

Energy Reports

Provided in Cooperation with:
Elsevier

Suggested Citation: Cao, Yan; Li, Yiqing; Zhang, Geng; Kittisak Jermsittiparsert; Razmjooy, Navid (2019) : Experimental modeling of PEM fuel cells using a new improved seagull optimization algorithm, Energy Reports, ISSN 2352-4847, Elsevier, Amsterdam, Vol. 5, pp. 1616-1625, https://doi.org/10.1016/j.egyr.2019.11.013

Energy Reports 5 (2019) 1616–1625

Contents lists available at ScienceDirect

Energy Reports

journal homepage: www.elsevier.com/locate/egyr

Research paper

Experimental modeling of PEM fuel cells using a new improved seagull optimization algorithm

Yan Cao [a], Yiqing Li [a], Geng Zhang [a], Kittisak Jermsittiparsert [b,*], Navid Razmjooy [c]

[a] School of Mechatronic Engineering, Xi'an Technological University, Shaanxi 710021, China
[b] Social Research Institute, Chulalongkorn University, Bangkok 10330, Thailand
[c] Department of Electrical Engineering, Tsfresh University, Tafresh, Iran

ARTICLE INFO

Article history:
Received 1 August 2019
Received in revised form 24 October 2019
Accepted 6 November 2019
Available online 12 November 2019

Keywords:
Seagull optimization algorithm
Lévy flight
Proton exchange membrane fuel cells
Modeling

ABSTRACT

This study proposes an optimal model to design and simulate the proton exchange membrane fuel cell (PEMFC) systems. The purpose of this paper is to present an improved version of seagull optimization algorithm for optimal parameter identification of the PEMFC stacks. The new algorithm uses the Lévy flight mechanism to give faster convergence rates. The sum of the squared error between the empirical values and achieved optimal model is analyzed based on two empirical PEMFC models including BCS 500-W and NedStack PS6. This analysis is performed to show the potential of the presented method by considering different conditions. Simulation results are compared with several optimization algorithms and show the algorithm's superiority in terms of the solutions quality and the convergence speed.

1. Introduction

Renewable energy refers to a variety of energy sources that, unlike non-renewable (fossil fuels), have the potential to be renewed by nature in a short period of time (Ahadi et al., 2015; Aghajani and Ghadimi, 2018; Mirzapour et al., 2019). Natural energy storage on Earth is coming to an end, and the resources that human beings have used to date will sooner or later be over. The only way to save on future generations and the survival of humanity is taking refuge in renewable energy resources.

Renewable energy is the energy that comes from recyclable or renewable resources and can be replaced by natural resources. This kind of energy has a much less environmental impact than fossil fuels which make them more popular toward fossil fuels. One of the potential renewable energy resources with high advantage like high performance energy conversion and greater environmental compatibility is fuel cell (Ghadimi, 2012; Abbaspour et al., 2016; Longo et al., 2019; Technology, 2019; Wang et al., 2019).

The increasing demand for energy and the limitation of natural energy sources have led researchers into study on fuel cells. Although there are still problems with fuel cell, they have advantages over non-polluting energy, high energy conversion efficiency, noise-free operation, and high reliability compared to other energy-generating products, and hopes to be one of the most important sources of clean energy for household and transportation purposes in the future.

The market for fuel cell power generators is very large and includes government, military and industrial applications. It is also used as a backup force in emergencies in telecommunications, medical industries, offices, hospitals, large hotels and computer systems (Noori et al., 2016). The fuel cells are relatively quiet and silent, so they are suitable for local power generation. In addition to reducing the need to expand the distribution network, the heat generated from these plants can be used to heat and produce steam.

Unlike other energy converters, fuel cells are not limited to use a particular power source and are capable of using different fuels such as methanol, ethanol, hydrogen, natural gas, propane and gasoline (Dicks and Rand, 2018; Choudhary and Sahu, 2019). Fuel cells, because of the ability to be portable, are widely used in mobile and portable applications such as UAVs and electric vehicles (Karimi et al., 2012; Mekhilef et al., 2012; Ijaodola et al., 2019).

Among several kinds of fuel cells, proton exchange membrane fuel cells (PEMFCs) are considered as a satisfied model which is because of its fast start-up, low operating temperature, and high efficiency (Hames et al., 2018; Taner, 2018). Polymer fuel cells are high power generators that can achieve a 40%–50% electrical efficiency in different power scales. They have also an operating temperature between 30 °C and 100 °C.

The basis for energy conversion in polymer fuel cells is the thermal reaction between oxygen and hydrogen in the air. The result of this reaction is electricity, heat and distilled water.

* Corresponding author.
E-mail address: kittisak.j@chula.ac.th (K. Jermsittiparsert).

https://doi.org/10.1016/j.egyr.2019.11.013
2352-4847/

Nomenclature

N_{nc}	Aumber for series connected cells of the PEMFC
E_{op}	Activation over-potential of the cells
E_{ops}	Over-potential saturation in cells
T_{PEM}	Operating cell temperature
P_H	Partial pressure of the H_2
P_{O_2}	Partial pressure of the O_2
P_{H_2O}	Partial pressure of the H_2O
I_{PEM}	Operating current of the PEMFC
C_{H2}	Hydrogen saturation
C_{O2}	Oxygen saturation
l	Thickness for the membrane
λ	Tunable parameter
β	Parametric coefficient
J_{max}	Maximum value of J
E_{oc}	Open circuit potential condition per cell
E_O	Ohmic voltage drop in each cell
S	Membrane surface
R_{hc}	Vapor relative humidity at cathode
R_{ha}	Vapor relative humidity at anode
P_a	Inlet pressure for the anode
P_c	Inlet pressure for the cathode
R_m	Membrane resistance
R_c	Connections resistance
β_i	Experimental coefficients
ρ_m	Membrane resistivity
J	Real current density

Advantages of polymer fuel cell, such as lower weight and the possibility of the system's renewability in a closed and independent battery cycle, have attracted research on replacing the polymer fuel cell system with the use of batteries in satellites.

For more realizing and design of PEMFCs, we need to perform a reliable model for them. PEMFC have different features such as dynamic models of the system, empirical data from the experiments that can be utilized for modeling and steady-state stability (Sun et al., 2015; Ge et al., 2018; El-Hay et al., 2019). There are several approaches for modeling PEMFC in the literatures.

In 1991, Springer et al. proposed a one-dimensional steady-state model of a PEMFC (Springer et al., 1991). The model was based on isothermal parameterization. In 2010, Caux et al. proposed a state-space model for identification of fuel cells in EVs (Caux et al., 2010). The method used energy management in HEVs. They finally work on temperature and gas flows control of the fuel cell.

In 2014, Panagiotis et al. proposed two dynamical models based on semi-empirical formulas and the electrical equivalent for PEMFC stack (Papadopoulos et al., 2014). Furthermore, the model was improved based on transfer function and semi-empirical equations. The main objective was to design a parametric analysis model for models capability.

In 2017, Solsona et al. presented an empirically validated model for a low-temperature PEMFC along with a humidifier (Solsona et al., 2017). They also utilized a control strategy model based on Nafion® membrane. Simulation results were compared with the Experimental results.

In 2017, a real-time model for PEMFC was presented by Kumar et al. They studied the modality of the method by different validation such as ARX and ARMAX (Kumar et al., 2018). They used MATLAB platform for system identification. To control the desired load current, PI and PID controllers were employed. In addition, several research works have been established on the modeled PEMFC (Bao and Bessler, 2015; Solsona et al., 2017).

However using aforementioned methods for modeling are useful for designing and analyzing the fuel cells, there is some depletion to these methods. Classic methods are based on considering all physical concepts of the fuel cells such as power, thermodynamics, momentum's conservation to achieve a precise thermal model for anything that happens in them which makes the modeling progress complicated.

We also know that all the uncertain processes which happen in the system cannot be modeled by the analytical modeling. This subject hardens using this type of modeling, especially in the practical operations. Meanwhile, for enhancing the accuracy of the model to achieve a close performance model from the actual PEMFC, it is important to reach the best parameter values of the system model.

Recently, the applications of bio-inspired meta-heuristic algorithm for different fields have been extensively increasing (Holland, 1992; Razmjooy and Ramezani, 2014; Razmjooy et al., 2016; Bagheri et al., 2018).

There are great deals of research works about the applications of bio-inspired optimization methods for parameter identification in the PEMFCs.

For example, particle swarm optimization (Li et al., 2010), Multi-verse optimizer (Fathy and Rezk, 2018), Genetic algorithm (Ariza et al., 2018), dragonfly algorithm (Hamal et al., 2018), differential evolution algorithm (Sun et al., 2015), etc.

In 2018, Mamaghani (Mamaghani et al., 2018) proposed a multi-objective procedure for an HT-PEM fuel cell utilized in a micro combined heat and power system. Various optimization methods were performed to find the optimal value of a defined multi-objective function. The method determined the optimal operating parameters and their corresponding efficiency indices. For the multi-objective optimization, electrical and thermal efficiencies have been utilized. The results showed that during the optimization, the electrical performance of the net is up to 32.3% and its thermal efficiency is higher than 61.1%.

Literature review show that utilizing optimization algorithms gives better results for the PEMFC identification. The main objective is that they can escape from the local minimum which leads them to obtain global optimum (Razmjooy and Ramezani, 2014; Namadchian et al., 2016; Razmjooy et al., 2016).

Seagull Optimization Algorithm (SOA) is a newly meta-heuristic technique that is proposed by Dhiman and Kumar (Dhiman and Kumar, 2019). The simplicity of SOA by less parameters and also its easy to implement feature make it applicable for different works. However, sometimes SOA trapped into the local optima. In this study, a new developed version of the SOA algorithm has been used for solving the nonlinear modeling problem of the PEMFCs identification problem.

2. Mathematical model of PEMFC

There are different models for PEMFCs which have been given based on the thermodynamic and the chemical aspects (Luo et al., 2015; Razmjooy et al., 2018). A fuel cell includes an electrolyte membrane, an anode (negative charge electrode), and a cathode (positive charge electrode). Hydrogen is ionized in the anode, producing electrons and protons. The electrons are sent to an external circuit and generate the current, and hydrogen protons pass through the membrane by transferring molecules to other molecules. In cathode, oxygen synthesizes with the electrons from the external circuit and the protons from the anode, generating heat and water. Both the cathode and anode include

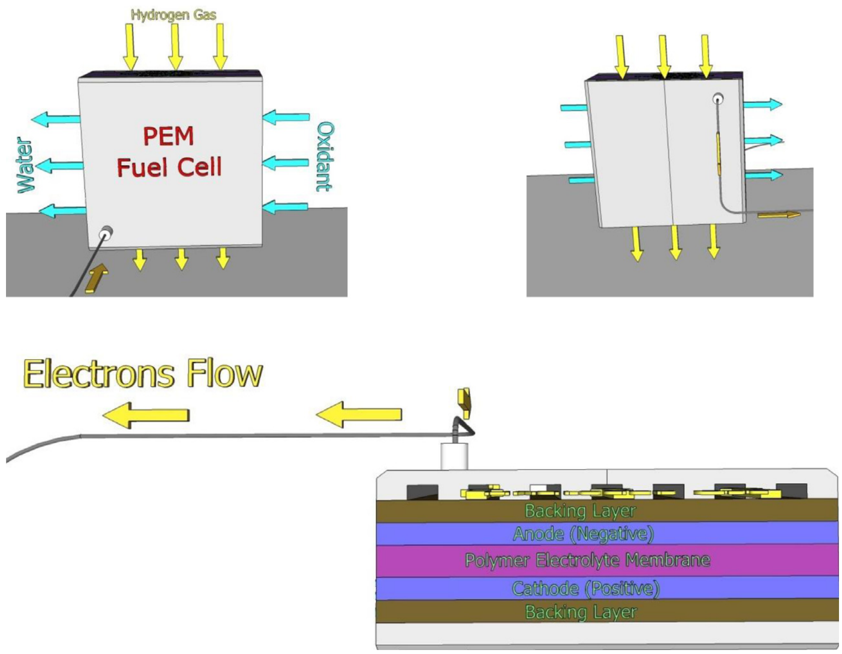

Fig. 1. The model of PEMFC stack.

catalysts to accelerate the electrochemical reaction. Fig. 1 shows the chemical reactions of the anode and cathode in the fuel cell.

The main purpose of the presented technique is to parameter identification of the PEMFCs using a new improved version of the Balanced Seagull Optimization Algorithm.

The cost function here is the error between achieved value of the designed model and the values obtained from the empirical values measured for the voltage data. Here, two empirical case studies are applied to show the efficiency of the presented modified BSOA through essential comparisons.

By considering entropy and irreversibility losses in a single PEMFC stack, the nominal output voltage is in the range 0.9 to 1.23 V. Therefore, to use the PEMFC stack in applications, a large number of them are combined with together in series.

Due to the activation voltage in PEMFC stacks, the current–voltage polarization curve falls down with a high slope, and then Ohmic resistive voltage drops make the curve to slowly falls down.

From (Corrêa et al., 2004; Aouali et al., 2017), the mathematical model of the total output voltage for PEMFC stack is formulated as follows:

$$V_o = N_{nc}\left(E_{oc} - E_{op} - E_O - E_{ops}\right) \tag{1}$$

where, N_{nc} represents the number for series connected cells of the PEMFC, E_{oc} is the open circuit potential condition per cell, E_{op} is the activation over-potential of the cells, E_O describes the Ohmic voltage drop in each cell, and E_{ops} is the over-potential saturation in cells.

To model the open circuit voltage of the PEMFC which is so-called reversible voltage, Nernst equation for this hydrogen/oxygen fuel cell has been utilized based on standard-state entropy change (Mann et al., 2000; Chen and Wang, 2019),

$$E_{oc} = 1.23 - 8.5\times10^{-4}\left(T_{PEM} - 298.15\right) + 4.31\times10^{-5} \times T_{PEM} \times ln\left(P_{H_2}\sqrt{P_{O_2}}\right) \tag{2}$$

where,

$$P_{O_2} = R_{hc}\times P_{H_2O}\left[\frac{1}{\frac{R_{hc}\times P_{H_2O}}{P_c}\times e^{\frac{1.635 I_{PEM}/A}{T^{1.334} I_{PEM}}}} - 1\right] \tag{3}$$

$$P_{H_2} = \frac{R_{ha}\times P_{H_2O}}{2}\left[\frac{1}{\frac{R_{ha}\times P_{H_2O}}{P_a}\times e^{\frac{1.635 I_{PEM}/A}{T^{1.334} I_{PEM}}}} - 1\right] \tag{4}$$

$$\log_{10}\left(P_{H_2O}\right) = 2.95\times10^{-2}T_c - 9.18\times10^{-5}T_c^2 + 1.4\times10^{-7}T_c^3 - 2.18 \tag{5}$$

$$T_c = T_{PEM} - 273.15 \tag{6}$$

The reference temperature value during the operating variations is considered 25 °C (77 °F).

The mathematical model of the activation over-potential is formulated below:

$$E_{op} = -\left[\gamma_1 + \gamma_2 T_{PEM} + \gamma_3 T_{PEM}\ln\left(C_{O_2}\right) + \gamma_4 T_{PEM}\ln\left(I_{PEM}\right)\right] \tag{7}$$

where,

$$\gamma_2 = 2.9\times10^{-3} + 2.1\times10^{-4}\ln(A) + 4.3\times10^{-5}\ln(C_{H_2}) \tag{8}$$

and C_{O_2} represents the oxygen saturation in the cathode's catalytic interface (mol/cm^3) and is achieved as follows:

$$C_{O_2} = \frac{P_{O_2}}{5.1\times10^6}\times e^{\frac{498}{T_{PEM}}} \tag{9}$$

The hydrogen saturation in the cathode's catalytic interface (mol/cm^3) is equal to:

$$C_{H_2} = \frac{P_{H_2}}{1.1\times10^6}\times e^{\frac{-77}{T_{PEM}}} \tag{10}$$

And the Ohmic voltage drop in the cells is formulated as follows:

$$E_O = I_{PEM}(R_m + R_c) \tag{11}$$

where,

$$R_m = \rho_m l S^{-1} \tag{12}$$

$$\rho_m = \frac{181.6\left[0.062\left(\frac{T_{PEM}}{303}\right)^2\left(\frac{I_{PEM}}{S}\right)^{2.5} + 0.03\left(\frac{I_{PEM}}{S}\right) + 1\right]}{\left[\lambda - 0.063 - 3\left(\frac{I_{PEM}}{S}\right)\right]\times e^{\frac{T_{PEM}-303}{T_{PEM}}}} \tag{13}$$

And, the over-potential saturation (E_{ops}) in cells is as follows:

$$E_{ops} = -\beta ln\left(1 - \frac{J}{J_{max}}\right) \tag{14}$$

where, T_{PEM} represents the operating cell temperature (K), P_H, P_{O_2}, and P_{H_2O} describe the partial pressure of the H_2, O_2 and H_2O, respectively. S describes the membrane surface (cm^2), R_{hc} and R_{ha} are the vapor relative humidity at cathode and anode, respectively, P_a and P_c represent the inlet pressure for the anode and the cathode, I_{PEM} represents the operating current of the PEMFC, C_{H2} and C_{O2} are the hydrogen and oxygen (mol/cm^3) saturation, R_m and R_c are the membrane resistance and the connections resistance, I is the thickness for the membrane, β_i describes the experimental coefficients, λ is tunable parameter, ρ_m is the membrane resistivity, β describes a parametric coefficient, J represents the real current density, and J_{max} is the maximum value of J.

By considering the aforementioned formulations, six parameters are need to be clarified which are not given by the manufacturer's datasheet.

In this condition, to achieve a satisfied model of PEMFCs, accurate values for the parameters are required. The six undetermined parameters here are β_1, β_2, β_3, β_4, β, $R_{c,\lambda}$.

In this study, we will try to achieve optimized values for the parameters by considering their constraints. A motivation of the algorithm is to use a new improved version of the recently introduced Balanced Seagull Optimization Algorithm to enhance the convergence speed op the algorithm.

3. Balanced seagull optimization algorithm (BSOA)

Seagulls (scientific name: Larus minutus) are among the birds of the coastal environments that have lived on Earth for about thirty million years and are present on almost all parts of the planet. Their wings are tall and their hind legs have evolved to move in water. However fish is the main food source of Seagulls, they also feed on insects, reptiles, amphibians, earthworms, and moles. In other words, seagulls are omnivorous. Seagulls are very smart birds that live for about 10 to 15 years (Trotter, 2019).

They live in large groups and have different voices to communicate with their band members. One of their strangest behaviors is that they are steal food from the grip of other birds, animals and even humans. They also use other techniques for hunting. For example, they attract fish with a bread crumbs or create a rain shower sound with their feet to drag. In general, seagulls live in swarm. Another capability is their specific behavior in migration.

Migration is the movement of seagulls to the south in the fall and northwards in the spring or moving from the ground to the heights or from coast to coast to survive from winter conditions and to achieve the most abundant food sources which provides enough easement (La Sorte et al., 2016). This mechanism is considered as a seasonal behavior of seagulls to move from one place to another to achieve a wide range of wealthy food sources to provide adequate energy (Avise, 2017). This process is illustrated below:

- Migration starts by traveling a swarm of seagulls. To avoid from collisions, their initial positions are different from each other.
- They benefit from their swarm experience, i.e. they attempts to move in the direction of the best survival to achieve the lowest cost value.

Generally, seagulls attack to the migrating birds over the sea. This process is performed by the spiral natural shape behavior of them during attacking.

In the following, the model of seagulls for Seagull Optimization Algorithm (SOA) is discussed.

3.1. Migration (exploration)

Migration behavior simulates the seagulls swarm moving toward the positions. To do so, three conditions should be satisfied:

(A) Collisions Avoidance: To avoid the collision among neighbor seagulls, a model is defined by additional variable A for updating the new position of the considered seagull (search agent):

$$\vec{P}_N = A \times \vec{P}_c\,(i)\,, \tag{15}$$
$$\text{i} = 0, 1, 2, \ldots, \text{Max(i)}$$

where, $\vec{P}_N$ describes the position that prevent from colliding with the other search agent, $\vec{P}_c(i)$ is the position of the candidate in the present iteration (i), and A describe the motion behavior of the search agent in the search space and is modeled as follow:

$$A = f_c - \left(i \times \left(\frac{f_c}{Max(i)}\right)\right) \tag{16}$$

where, i describes the iteration, f_c represents the frequency control of variable A in the interval $[0, f_c]$.

(B) Using the other neighbor's experience: After collision avoidance form the neighbors, the candidates try to proceed into the direction of the best neighbor (best solution).

$$\vec{d}_e = B \times \left(\vec{P}_b\,(i) - \vec{P}_c(i)\right) \tag{17}$$

where, $\vec{d}_e$ describe the candidate positions $\vec{P}_c(i)$ toward the best fit candidate $\vec{P}_b\,(i)$. The coefficient B is a random value that makes trade-off between exploitation and exploration. B is achieved as follows:

$$B = 2 \times A^2 \times R \tag{18}$$

where, R describes a random value between 0 and 1.

(C) Move toward the best solution (search agent): finally, search agents update their position based on the best solution by the following formula:

$$\vec{D}_e = \left|\vec{P}_N + \vec{d}_e\right| \tag{19}$$

where, $\vec{D}_e$ describes the difference between the seagulls and the best cost.

3.2. Attacking (exploitation)

During migration, seagulls can continuously vary the attack's angle and speed. The position of them in can be kept in the air with the help of their weight and wings.

During the attack process, seagulls they move spiral in the air in x, y, and z planes as follows:

$$\hat{x} = r \times cos(t) \tag{20}$$

$$\hat{y} = r \times sin(t) \tag{21}$$

$$\hat{z} = r \times t \tag{22}$$

where, t describes a random value in the interval 0 and 2π and r declares the radius of the spiral turns and is formulated as follows:

$$r = \alpha \times e^{\beta t} \tag{23}$$

where, e describes the natural logarithm base, and α and β represent the shape of the spiral. The new position of seagulls is updated by the following formula:

$$\vec{P}_c\,(i) = \left(\vec{D}_e \times \hat{x} \times \hat{y} \times \hat{z}\right) + \vec{P}_b\,(i) \tag{24}$$

where, $\vec{P}_c\,(i)$ keeps the best results.

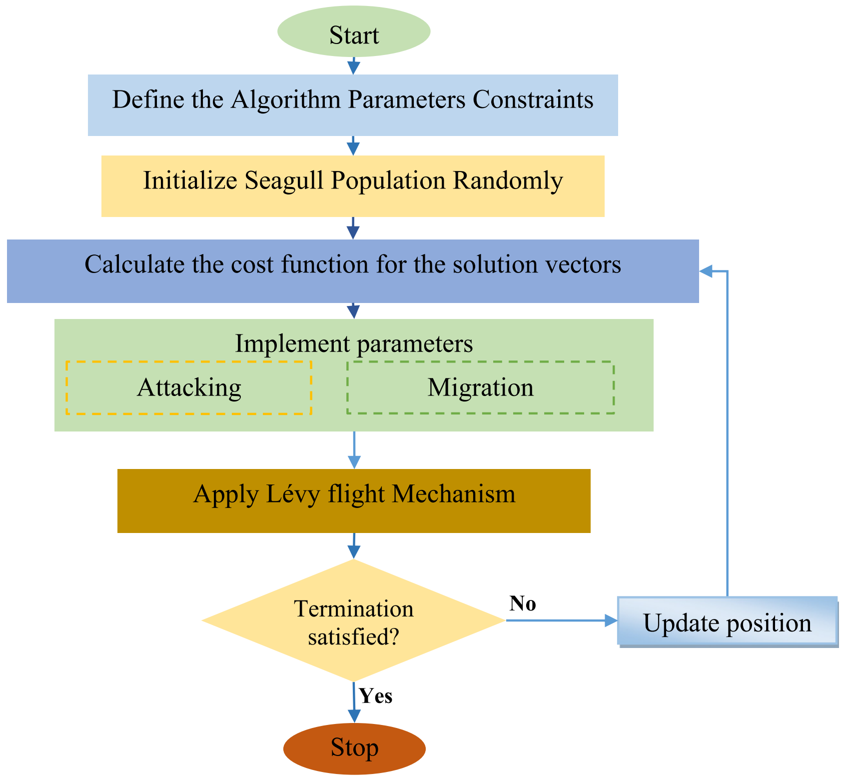

Fig. 2. The flowchart diagram of the proposed BSOA.

3.3. The balanced SOA

In this section, Lévy flight have been used for improving the proposed SOA. This mechanism is utilized to further relieve the premature convergence drawback, which are the core disadvantage of the SOA. Lévy flight (LF) provides a random walk mechanism to proper control of local search (Choi and Lee, 1998). This mechanism is represented as follows:

$$Le\,(w) \approx w^{-1-\tau} \tag{25}$$

$$w = \frac{A}{|B|^{1/\tau}} \tag{26}$$

$$\sigma^2 = \left\{ \frac{\Gamma(1+\tau)}{\tau\Gamma((1+\tau)/2)} \frac{\sin(\pi\tau/2)}{2^{(1+\tau)/2}} \right\}^{\frac{2}{\tau}} \tag{27}$$

where, $0 < \tau \leq 2$, $A \sim N(0, \sigma^2)$ and $B \sim N(0, \sigma^2)$, $\Gamma\,(.)$ is Gamma function, w describes the step size, τ represents Lévy index, , A/B $\sim$ N(0, σ 2) means that the samples generate from a Gaussian distribution in which mean is zero and variance is σ^2, respectively.

In this paper, based on (Li et al., 2018), $\tau = 3/2$.

Based on the aforementioned mechanism, the new improved part for update the solution of SOA is:

$$\vec{D}_{el} = \vec{D}_e + \left|\vec{P}_N + \vec{d}_e\right| \times \mathrm{Le}(\delta) \tag{28}$$

where, $\vec{D}_{el}$ represents the new position of search agent $\vec{D}_e$.

For guaranteeing the best solution candidates, fitter agents are kept:

$$\vec{D}_{el} = \begin{cases} \vec{D}_{el} & F\left(\vec{D}_{el}\right) > F(\vec{D}_e) \\ \vec{D}_e & otherwise \end{cases} \tag{29}$$

The flowchart of the presented BSOA is given in Fig. 2.

4. Validation of the proposed balanced SOA

For validation of the balanced SOA, four standard benchmarks have been studied. The results of the presented BSOA are compared with some different state of the art algorithms including particle swarm optimization algorithm (PSO) (Bansal, 2019), world cup optimization algorithm (WCO) (Razmjooy et al., 2016), genetic algorithm (GA) (Holland, 1992), fluid search optimization algorithm (FSO) (Dong and Wang, 2018), and the original seagull optimization algorithm (SOA) (Dhiman and Kumar, 2019). The simulations have been applied to a laptop with MATLAB R2017b platform with processor Intel® CoreTM i7-4720 HQ CPU@2.60 GHz with 16 GB RAM. The equation and the constraints of the studied benchmark are illustrated in Table 1.

The results of the introduced benchmarks are given in Table 2. Here, the mean deviation (MD) and the standard deviation (SD) values of the compared methods are illustrated.

Simulation results from Table 2 show that the proposed BSOA gives promising results toward the other methods, especially the original SOA.

Fig. 3 shows the convergence curves for f1(A), f2(B), f3(C), and f4(D).

5. Objective function for PEMFC and its constraints

The PEMFC model parameters are optimized by the proposed BSOA to predict an optimal model which matches with the actual outputs of the system as much as possible.

By considering the aforementioned formulations and parameters, after determining the parameters ($\beta_1, \beta_2, \beta_3, \beta_4, \beta, R_{c,\lambda}$), we can predict the output voltage for any definite input current. In this study, the sum of squared error (SSE) has been adopted to show the similarity of the output voltage for the model and the empirical result.

Table 1
The utilized benchmarks for efficiency analysis.

Benchmark	Formula	Constraints	Dimension
Rastrigin	$f_1(x) = 10D + \sum_{i=1}^{D} \left(x_i^2 - 10\cos(2\pi x_i)\right)$	[−512, 512]	30–50
Rosenbrock	$f_2(x) = \sum_{i=1}^{D-1} \left(100\left(x_i^2 - x_{i+1}\right) + (x_i - 1)^2\right)$	[−2.045, 2.045]	30–50
Ackley	$f_3(x) = -20exp\left(-0.2\sqrt{\frac{1}{D}\sum_{i=1}^{D} x_i^2}\right) - exp\left(\frac{1}{D}\sum_{i=1}^{D} cos\,(2\pi x_i)\right) + 20 + e$	[−10, 10]	30–50
Sphere	$f_4(x) = \sum_{i=1}^{D} x_i^2$	[−512, 512]	30–50

Table 2
The results of the efficiency analysis by considering 30-dimensions.

Benchmark		BSOA	SOA (Dhiman and Kumar, 2019)	GA (Holland, 1992)	PSO (Bansal, 2019)	WCO (Razmjooy et al., 2016)	FSO (Dong and Wang, 2018)
f_1	MD	0.00	2.11	70.61	74.24	2.19	3.42
	SD	0.00	3.26	1.66	8.96	4.35	3.27
f_2	MD	6.32	6.53	35.41	200.1	13.16	8.64
	SD	3.85	1.96	27.15	59.00	4.62	2.56
f_3	MD	0.00	1.63e−17	3.19e−2	8.26	3.14e−3	4.46e−16
	SD	0.00	0.00	2.14e−2	1.19	1.12e−3	0.00
f_4	MD	0.00	3.57e−13	1.15e−4	8.27e−4	6.19e−9	1.55e−12
	SD	0.00	8.97e−18	3.14e−5	5.12e−4	3.28e−9	5.37e−17

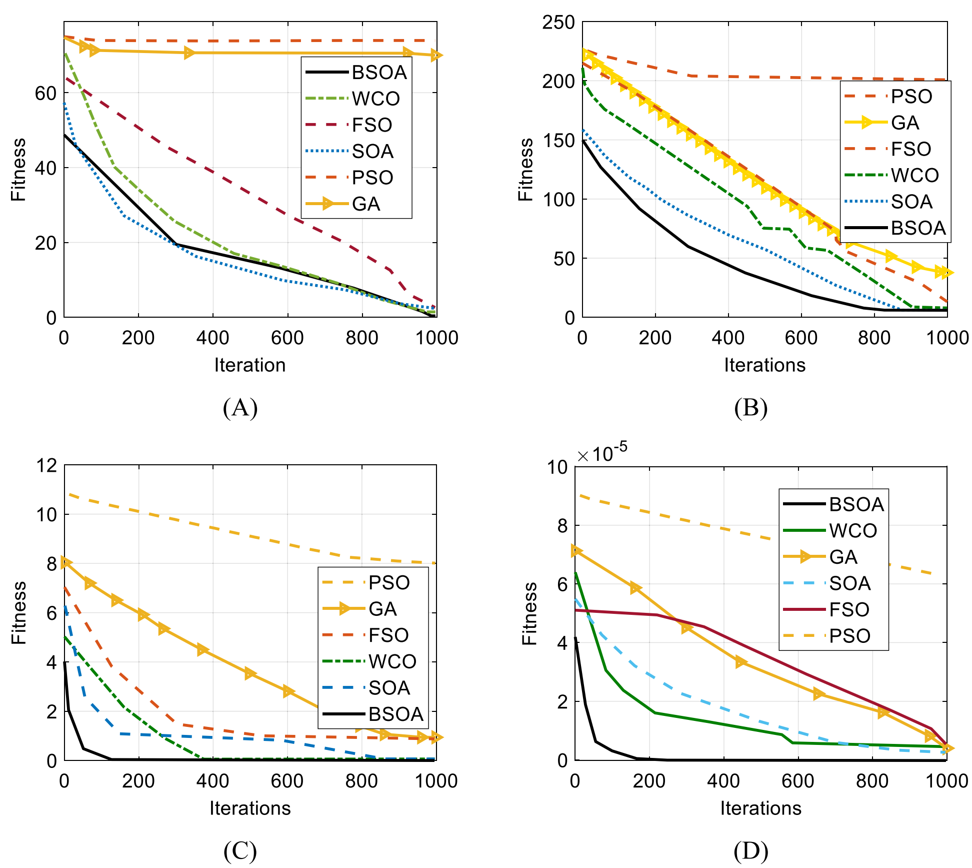

Fig. 3. Convergence curves for f1(A), f2(B), f3(C), and f4(D).

Therefore, the cost function is assumed as follows:

$$F_{SSE} = \min(SSE) = min\left\{\sum_{i=1}^{n}(V_e(i) - V_o(i))^2\right\} \tag{30}$$

where, n represents the number of measured points, i describes the number of iteration, and V_e and V_o are the empirical and the evaluated voltage stack of the PEMFC.

And the constraints for this function are declared in the following:

$$s.t.\begin{cases}\beta_{i,min} \le \beta_i \le \beta_{i,max}\\ \beta_{min} \le \beta_i \le \beta_{max}\\ R_{c,min} \le R_c \le R_{c,max}\\ \lambda_{min} \le \lambda_i \le \lambda_{max}\end{cases} \tag{31}$$

where, $\beta_{i,min}$ and $\beta_{i,max}$ represent the lower and the higher ranges for the empirical results, β_{min} and β_{max} describe the lower and the higher bounds for the parameters of the model, $R_{c,min}$ and $R_{c,max}$ are the lower and the higher ranges of the resistance for the cell connections, and λ_{min} and λ_{max} are lower and higher ranges of the water content.

6. Simulation results

To efficiency analysis of the proposed method, two practical case studies including BCS 500-W and NedStack PS6 have been adopted.

Some different optimized algorithms are also employed to fair efficiency analysis of the presented technique by assuming the same constraints from Priya et al. (2015), Ali et al. (2017) and El-Fergany (2017). The lower and the upper ranges for the studied six undetermined PEMFC parameters are given below:

$$\begin{cases}-1.2 \le \beta_1 \le -0.85\\ 3.6e-5 \le \beta_3 \le 9.8e-5\\ -2.6e-4 \le \beta_4 \le -9.54e-5\\ 1.4e-2 \le \beta \le 0.5\\ 0.1 \le R_c \le 0.8\\ 13 \le \lambda_i \le 23\end{cases}$$

The relative humidity of vapors for both anode and cathode are assumed 1.00.

6.1. Case study 1: NedStack PS6

In this part, for evaluating efficiency of the algorithm, a NedSstack PS6 of 6 kW rated power PEMFC system has been studied. For simulating this case study, its information is collected from El Monem et al. (2014) and Technology (2019). The required parameters of the NedStack PS6 is given in Table 3. By using the proposed BSOA for determining the best solution for the six undetermined parameters of NedStack PS6 system along with computed β_2, the final optimal values for the identified PEMFC model are given to shows the minimum value for the SSE overall 50 independent runs. The simulation results and elapsed time of the proposed BSOA compared with Seeker optimization (SO) algorithm (Dai et al., 2011), grasshopper optimiser (GHO) (El-Fergany, 2017), Salp Swarm Optimizer (SSO) (El-Fergany, 2018), and standard seagull optimization algorithm (SOA) and the results are given in Tables 4 and 5.

Fig. 4 shows the convergence diagram of the presented BSO algorithm on the NedS stack PS6 of 6 kW system.

Results show that the minimum SSE value after convergence is 2.18 which belong to the proposed method. It is clear that after 22 iterations, the SSE satisfied its minimum value that shows a high convergence characteristic than the standard SOA which needs 80 iterations.

Running time for the proposed method and the compared methods are illustrated in Table 5. Experimental results show that using the presented BSOA algorithm gives the best solution for the problem based on its improved convergence feature.

The current–voltage curve of the NedStack for the experimental curve and model curve based on BSOA is shown in Fig. 5.

Fig. 5 shows that the proposed BSOA gives satisfying precision to achieve the optimal fitting and by giving proper values for the undetermined parameters.

To better performance analysis of the algorithm, different conditions of partial pressures and the cell temperature are also studied. The current–voltage diagram for these variations is shown in Figs. 6 and 7.

Fig. 6 shows the partial pressure variations with 1/1 bar, 2/1.5 bar, and 3/2 bar. The results show that increasing the supply pressures of the P_{H2}/P_{O2} makes the stack output voltage increased.

Fig. 7 shows the constant cell temperature variations with 323 K, 343 K, and 363 K. The results show that increasing temperature make the stack output voltage increased.

Table 3
Required parameters of the NedStack PS6.

Parameter	Value	Unit
N_{cells}	65	–
A	240	cm^2
L	178	μm
T_{PEM}	343	K
Output voltage changes	[32, 60]	V
Output current changes	[0, 225]	A
Supply pressure changes	[0.5, 5]	bar

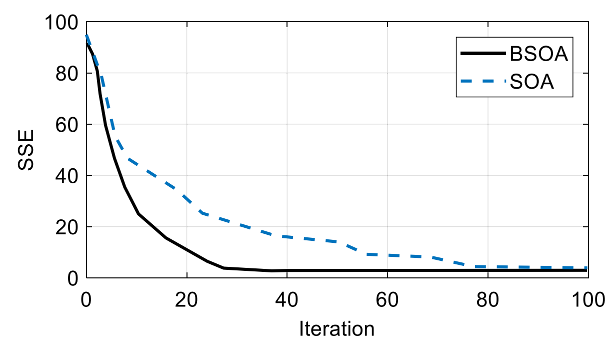

Fig. 4. The simulation results of SSE convergence on the NedS stack based on BSOA and SOA.

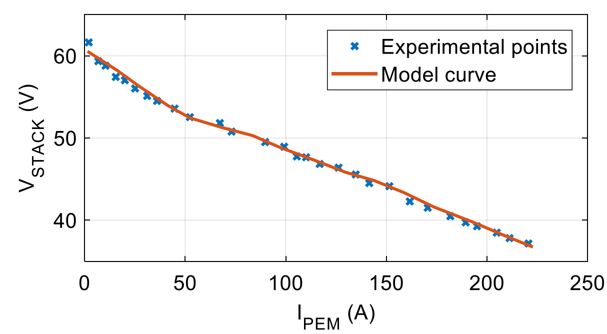

Fig. 5. The current–voltage curve for the NedStack.

Table 4
SSE validation for the NedStack PS6.

Parameter	Algorithm				
	BSOA	SOA	SO (Dai et al., 2011)	SSO (El-Fergany, 2018)	GHO (El-Fergany, 2017)
β_1	−0.89	−0.89	1.21	1.13	−0.96
β_2	3.42e−3	3.45e−3	3.38e−3	3.46e−3	3.41e−3
β_3	7.76e−5	7.52e−5	3.58e−5	4.59e−5	8.13e−5
β_4	−9.55e−5	−9.49e−5	−9.49e−5	−9.62e−5	−9.37e−5
λ	13.00	13.14	13.10	12.91	13.00
R_c	0.10	0.09	0.14	0.10	0.10
β	0.05	0.40	0.04	0.06	0.05
SSE	2.18	2.21	2.41	2.23	2.19

Table 5
Running time for the BSOA algorithm and the compared methods on the NedS stack.

Algorithm	BSOA	SOA	SO (Dai et al., 2011)	SSO (El-Fergany, 2018)	GHO (El-Fergany, 2017)
Elapsed time (s)	3.95	4.19	6.20	5.29	7.82

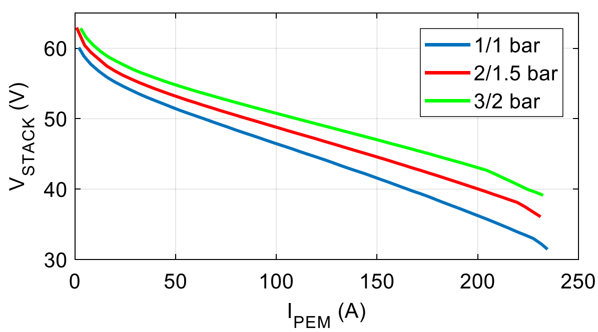

Fig. 6. The current–voltage curve characteristics of NedStack for pressure variations.

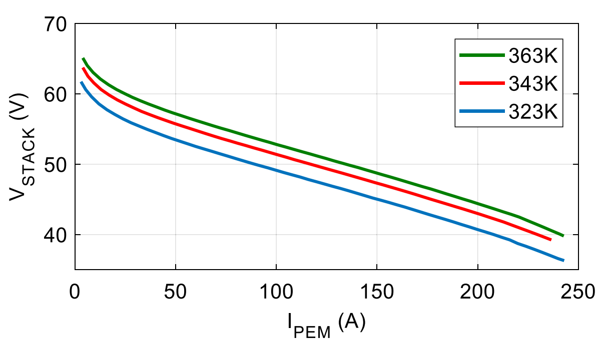

Fig. 7. The current–voltage curve characteristics of NedStack for varying temperatures.

6.2. Test case 2

This case study includes BCS PEMFC at a 500 W rated power with a 30 A maximum current. The model is made by American Company BCS Technologies (Co, 2001).

For simulating the BCS PEMFC stack, its information is collected from Corrêa et al. (2004). Table 3 illustrates the required parameters of the NedStack PS6 (see Table 6).

The simulation results and the running time of the proposed BSOA compared with Seeker optimization (SO) algorithm (Dai et al., 2011), grasshopper optimiser (GHO) (El-Fergany, 2017), Salp Swarm Optimizer (SSO) (El-Fergany, 2018), and standard seagull optimization algorithm (SOA) and the results are given in Tables 7 and 8.

Table 7 illustrates the simulation results of the optimal value selection for the voltage stack-based parameters based on the proposed BSOA compared with other methods on BCS PEMFC model for 100 independent runs.

Table 6
Required parameters of the NedStack PS6.

Parameter	Value	Unit
N_{cells}	32	–
A	64	cm^2
L	178	μm
TPEM	333	K
Partial pressures of H2	1	atm
Partial pressures of O2	0.21	atm
Output voltage changes	[32, 60]	V
Output current changes	[0, 225]	A
Supply pressure changes	[0.5, 5]	bar

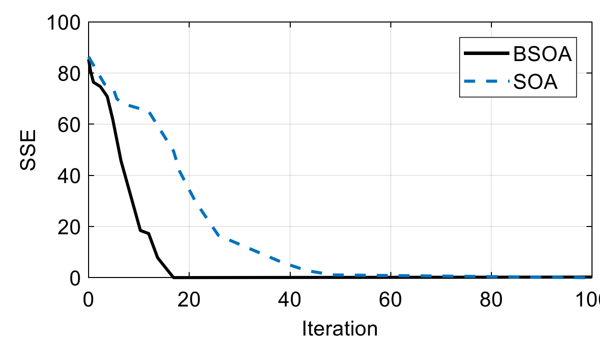

Fig. 8. The simulation results of SSE convergence on the BCS stack based on BSOA and SOA.

From Table 7, it is obvious that show utilizing the presented BSOA gives better efficiency with minor SSE value toward the others in 100 independent runs.

Fig. 8 shows the SSE convergence diagram of the proposed BSOA on the BCS PEMFC. From figure, it is observed that, like the earlier case study, the proposed method gives the minimum SSE value.

Fig. 8 shows the high speed of the proposed algorithm into the minimum SSE after 18 iterations.

Simulations results declare that the proposed BSOA gives the best speed among the other methods. This is illustrated in Table 8.

The current–voltage diagram of the BCS PEMFC for the experimental curve and model curve based on the presented BSOA is shown in Fig. 9.

Like the previous case study, the results declare that a satisfied fitting between the empirical voltage model and the data obtained by the proposed BSOA and shows high precision to achieve the optimized values for the undetermined parameters.

Table 7
SSE validation for the BCS PEMFC.

Parameter	Algorithm				
	BSOA	SOA	SO (Dai et al., 2011)	SSO (El-Fergany, 2018)	GHO (El-Fergany, 2017)
β_1	−0.81	−0.75	−1.02	−1.01	−0.79
β_2	5.17e−3	5.34e−3	5.14e−3	3.22e−3	4.12e−3
β_3	8.79e−5	9.15e−5	7.96e−5	5.45e−5	8.37e−5
β_4	−2.39e−4	−2.14e−4	−2.17e−4	−1.42e−4	−2.12e−4
λ	22.95	22.92	22.86	20.17	22.95
R_c	0.32	0.32	0.31	0.75	0.37
β	0.01	0.02	0.02	0.01	0.02
SSE	0.01	0.02	0.02	0.03	0.02

Table 8
Running time for the BSOA algorithm and the compared methods on the BCS PEMFC.

Algorithm	BSSO	SSO	SO (Dai et al., 2011)	SSO (El-Fergany, 2018)	GHO (El-Fergany, 2017)
Elapsed time (s)	3.75	4.94	6.28	5.13	6.95

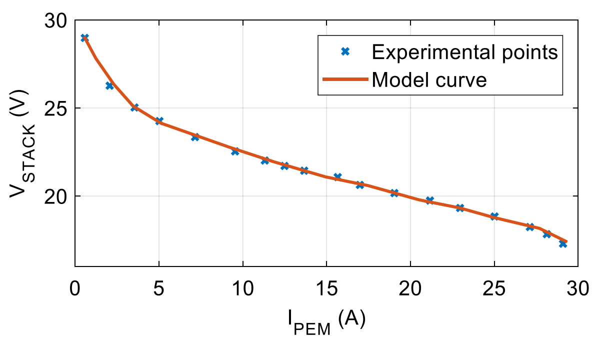

Fig. 9. The current–voltage curve for the BCS stack.

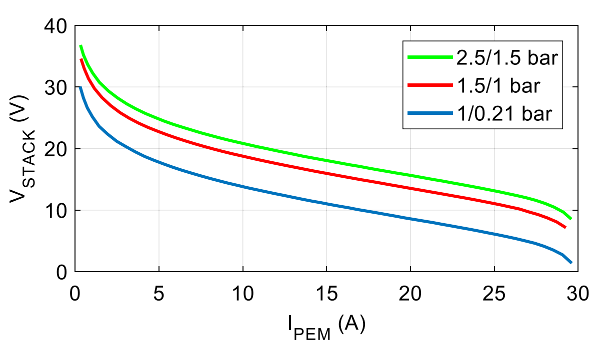

Fig. 10. The current–voltage diagram characteristics of BCS Stack for pressure variations.

In Figs. 10 and 11, the current–voltage diagram of the BCS PEMFC for different temperature and pressure values are plotted.

The variations of the partial pressure values for 2.5/1.5 bar, 1.5/1 bar, and 1/0.21 bar are shown in Fig. 10. It is obvious that increasing the supply pressures of the P_{H2}/P_{O2}, enhances the output voltage of the stack.

Fig. 10 shows the constant cell temperatures variations with for 373 K, 333 K, and 303 K in which increasing the temperature value, enhances the stack output voltage.

The results for both case studies give better performance for the proposed balanced SOA method compared with the other analyzed optimization algorithm in terms of both precision and convergence speed. Therefore, the results prove that using the proposed method is a promising method for parameter identification of the PEMFC with different conditions.

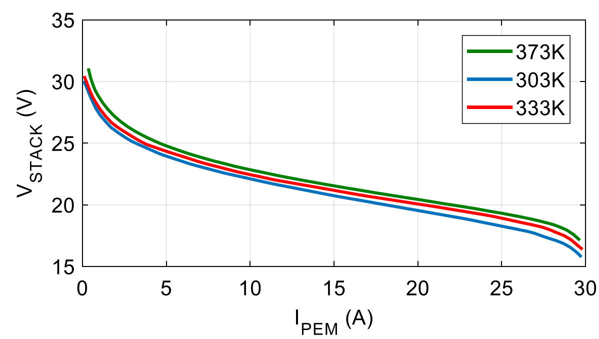

Fig. 11. The current–voltage diagram characteristics of BCS Stack for varying temperatures.

7. Conclusions

This study presents a new improved bio-inspired method for solving the nonlinear modeling problem of the PEMFCs identification problem. The method uses bio-inspired technique to guarantee the optimal values for modeling the complex nonlinear PEMFC systems. Here, a balanced version of the seagull optimization algorithm is presented. The BSOA algorithm uses Lévy flight mechanism that makes the standard seagull optimization algorithm to get better convergence. The BSOA was analyzed based on two empirical PEMFC types in comparison with some different optimization algorithms. Simulation results show that the proposed technique gives dynamic behavior of PEMFC output current/voltage properly and has effective performance.

Declaration of competing interest

The authors declare that they have no known competing financial interests or personal relationships that could have appeared to influence the work reported in this paper.

Acknowledgment

Thanks to Emate for language service.

References

Ahadi, A., Ghadimi, N., Mirabbasi, D., 2015. An analytical methodology for assessment of smart monitoring impact on future electric power distribution system reliability. Complexity 21 (1), 99–113.
Aghajani, G., Ghadimi, N., 2018. Multi-objective energy management in a micro-grid. Energy Rep. 4, 218–225.

Mirzapour, F., Lakzaei, M., Varamini, G., Teimourian, M., Ghadimi, N., 2019. A new prediction model of battery and wind-solar output in hybrid power system. J. Ambient Intell. Humaniz. Comput. 10 (1), 77–87.
Ghadimi, N., 2012. Genetically tuning of lead–lag controller in order to control of fuel cell voltage. Sci. Res. Essays 7 (43), 3695–3701.
Abbaspour, A., Khalilnejad, A., Chen, Z., 2016. Robust adaptive neural network control for PEM fuel cell. Int. J. Hydrogen Energy 41 (44), 20385–20395.
Longo, S., Cellura, M., Guarino, F., Brunaccini, G., Ferraro, M., 2019. Life cycle energy and environmental impacts of a solid oxide fuel cell micro-CHP system for residential application. Sci. Total Environ..
Technology, N.F.C., 2019. Nedstack fuel cell technology. from http://www.fuelcellmarkets.com/content/images/articles/ps6pdf.
Wang, H., Gaillard, A., Hissel, D., 2019. A review of DC/dc converter-based electrochemical impedance spectroscopy for fuel cell electric vehicles. Renew. Energy.
Noori, M.T., Ghangrekar, M., Mukherjee, C., 2016. V2o5 microflower decorated cathode for enhancing power generation in air-cathode microbial fuel cell treating fish market wastewater. Int. J. Hydrogen Energy 41 (5), 3638–3645.
Dicks, A., Rand, D.A.J., 2018. Fuel Cell Systems Explained. Wiley Online Library.
Choudhary, T., Sahu, M.K., 2019. Energy and exergy analysis of solid oxide fuel cell integrated with gas turbine cycle—A hybrid cycle. In: Renewable Energy and its Innovative Technologies. Springer, pp. 139–153.
Karimi, M., Imanzadeh, M., Farhadi, P., Ghadimi, N., 2012. Voltage control of PEMFC using a new controller based on reinforcement learning. Int. J. Inf. Electron. Eng. 2 (5).
Mekhilef, S., Saidur, R., Safari, A., 2012. Comparative study of different fuel cell technologies. Renew. Sustain. Energy Rev. 16 (1), 981–989.
Ijaodola, O., El-Hassan, Z., Ogungbemi, E., Khatib, F., Wilberforce, T., Thompson, J., Olabi, A., 2019. Energy efficiency improvements by investigating the water flooding management on proton exchange membrane fuel cell (PEMFC). Energy 179, 246–267.
Hames, Y., Kaya, K., Baltacioglu, E., Turksoy, A., 2018. Analysis of the control strategies for fuel saving in the hydrogen fuel cell vehicles. Int. J. Hydrogen Energy 43 (23), 10810–10821.
Taner, T., 2018. Energy and exergy analyze of PEM fuel cell: a case study of modeling and simulations. Energy 143, 284–294.
Sun, Z., Wang, N., Bi, Y., Srinivasan, D., 2015. Parameter identification of PEMFC model based on hybrid adaptive differential evolution algorithm. Energy 90, 1334–1341.
Ge, W., Qi, Z., Xue, C., Xu, M., 2018. Research on modeling of PEMFC based on fractional order subspace identification. In: 2018 37th Chinese Control Conference (CCC). IEEE.
El-Hay, E., M., El-Hameed, El-Fergany, A., 2019. Optimized parameters of SOFC for steady state and transient simulations using interior search algorithm. Energy 166, 451–461.
Springer, T.E., Zawodzinski, T., Gottesfeld, S., 1991. Polymer electrolyte fuel cell model. J. Electrochem. Soc. 138 (8), 2334–2342.
Caux, S., Hankache, W., Fadel, M., Hissel, D., 2010. PEM Fuel cell model suitable for energy optimization purposes. Energy Convers. Manage. 51 (2), 320–328.
Papadopoulos, P.N., Kandyla, M., Kourtza, P., Papadopoulos, T.A., Papagiannis, G.K., 2014. Parametric analysis of the steady state and dynamic performance of proton exchange membrane fuel cell models. Renew. Energy 71, 23–31.
Solsona, M., Kunusch, C., Ocampo-Martinez, C., 2017. Control-oriented model of a membrane humidifier for fuel cell applications. Energy Convers. Manag. 137, 121–129.
Kumar, P.A., Geetha, M., Chandran, K., Sanjeevikumar, P., 2018. PEM Fuel cell system identification and control. In: Advances in Smart Grid and Renewable Energy. Springer, pp. 449–457.
Bao, C., Bessler, W.G., 2015. Two-dimensional modeling of a polymer electrolyte membrane fuel cell with long flow channel. part II. Physics-based electrochemical impedance analysis. J. Power Sources 278, 675–682.
Holland, J.H., 1992. Genetic algorithms. Sci. Amer. 267 (1), 66–73.
Razmjooy, N., Ramezani, M., 2014. An improved quantum evolutionary algorithm based on invasive weed optimization. Indian J. Sci. Res. 4 (2), 413–422.
Razmjooy, N., Khalilpour, M., Ramezani, M., 2016. A new meta-heuristic optimization algorithm inspired by FIFA world cup competitions: Theory and its application in PID designing for AVR system. J. Control Autom. Electr. Syst. 27 (4), 419–440.
Bagheri, M., Sultanbek, A., Abedinia, O., Naderi, M.S., Naderi, M.S., Ghadimi, N., 2018. Multi-objective shark smell optimization for solving the reactive power dispatch problem. In: 2018 IEEE International Conference on Environment and Electrical Engineering and 2018 IEEE Industrial and Commercial Power Systems Europe (EEEIC/I & CPS Europe). IEEE.
Li, Q., Chen, W., Wang, Y., Liu, S., Jia, J., 2010. Parameter identification for PEM fuel-cell mechanism model based on effective informed adaptive particle swarm optimization. IEEE Trans. Ind. Electron. 58 (6), 2410–2419.
Fathy, A., Rezk, H., 2018. Multi-verse optimizer for identifying the optimal parameters of PEMFC model. Energy 143, 634–644.
Ariza, H., Correcher, A., Sánchez, C., Pérez-Navarro, Á., García, E., 2018. Thermal and electrical parameter identification of a proton exchange membrane fuel cell using genetic algorithm. Energies 11 (8), 2099.
Hamal, N.S., Isa, Z.M., Nayan, N.M., Arshad, M.H., Kajaan, N.A.M., 2018. Optimizing PEMFC model parameters using dragonfly algorithm: a performance study.
Mamaghani, A.H., Najafi, B., Casalegno, A., Rinaldi, F., 2018. Optimization of an HT-PEM fuel cell based residential micro combined heat and power system: A multi-objective approach. J. Clean. Prod. 180, 126–138.
Namadchian, A., Ramezani, M., Razmjooy, N., 2016. A new meta-heuristic algorithm for optimization based on variance reduction of guassian distribution. Majlesi J. Electr. Eng. 10 (4), 49.
Dhiman, G., Kumar, V., 2019. Seagull optimization algorithm: Theory and its applications for large-scale industrial engineering problems. Knowl.-Based Syst. 165, 169–196.
Luo, X., Wang, J., Dooner, M., Clarke, J., 2015. Overview of current development in electrical energy storage technologies and the application potential in power system operation. Appl. Energy 137, 511–536.
Razmjooy, N., Ramezani, M., Estrela, V.V., Loschi, H.J., do Nascimento, D.A., 2018. Stability analysis of the interval systems based on linear matrix inequalities. In: Brazilian Technology Symposium. Springer.
Corrêa, J.M., Farret, F.A., Canha, L.N., Simoes, M.G., 2004. An electrochemical-based fuel-cell model suitable for electrical engineering automation approach. IEEE Trans. Ind. Electron. 51 (5), 1103–1112.
Aouali, F.Z., Becherif, M., Ramadan, H.S., Emziane, M., Khellaf, A., Mohammedi, K., 2017. Analytical modelling and experimental validation of proton exchange membrane electrolyser for hydrogen production. Int. J. Hydrogen Energy 42 (2), 1366–1374.
Mann, R.F., Amphlett, J.C., Hooper, M.A., Jensen, H.M., Peppley, B.A., Roberge, P.R., 2000. Development and application of a generalised steady-state electrochemical model for a PEM fuel cell. J. Power Sources 86 (1–2), 173–180.
Chen, Y., Wang, N., 2019. Cuckoo search algorithm with explosion operator for modeling proton exchange membrane fuel cells. Int. J. Hydrogen Energy 44 (5), 3075–3087.
Trotter, S., 2019. Birds behaving badly: the regulation of seagulls and the construction of public space. J. Law Soc. 46 (1), 1–28.
La Sorte, F.A., Fink, D., Hochachka, W.M., Kelling, S., 2016. Convergence of broad-scale migration strategies in terrestrial birds. Proc. R. Soc. B 283 (1823), 20152588.
Avise, J.C., 2017. The Life of a Couple of Birds. from Aardvarks to Zooxanthellae. Springer, pp. 41–46.
Choi, C., Lee, J.-J., 1998. Chaotic local search algorithm. Artif. Life Robot. 2 (1), 41–47.
Li, X., Niu, P., Liu, J., 2018. Combustion optimization of a boiler based on the chaos and Levy flight vortex search algorithm. Appl. Math. Model. 58, 3–18.
Bansal, J.C., 2019. Particle Swarm Optimization. In: Evolutionary and Swarm Intelligence Algorithms, Springer, pp. 11–23.
Dong, R., Wang, S., 2018. New optimization algorithm inspired by fluid mechanics for combined economic and emission dispatch problem. Turk. J. Electr. Eng. Comput. Sci. 26 (6), 3305–3318.
Priya, K., Babu, T.S., Balasubramanian, K., Kumar, K.S., Rajasekar, N., 2015. A novel approach for fuel cell parameter estimation using simple genetic algorithm. Sustain. Energy Technol. Assess. 12, 46–52.
Ali, M., El-Hameed, M., Farahat, M., 2017. Effective parameters' identification for polymer electrolyte membrane fuel cell models using grey wolf optimizer. Renew. Energy 111, 455–462.
El-Fergany, A.A., 2017. Electrical characterisation of proton exchange membrane fuel cells stack using grasshopper optimiser. IET Renew. Power Gener. 12 (1), 9–17.
El Monem, A.A., Azmy, A.M., Mahmoud, S., 2014. Effect of process parameters on the dynamic behavior of polymer electrolyte membrane fuel cells for electric vehicle applications. Ain Shams Eng. J. 5 (1), 75–84.
Dai, C., Chen, W., Cheng, Z., Li, Q., Jiang, Z., Jia, J., 2011. Seeker optimization algorithm for global optimization: a case study on optimal modelling of proton exchange membrane fuel cell (PEMFC). Int. J. Electr. Power Energy Syst. 33 (3), 369–376.
El-Fergany, A.A., 2018. Extracting optimal parameters of PEM fuel cells using salp swarm optimizer. Renew. Energy 119, 641–648.
Co, B.T., 2001. Data sheet for a 500-W FC stack.